The Top Quark: Experimental Roots and Branches of Theory*

Elizabeth H. Simmons

1 Introduction

Even before the top quark was discovered by the CDF[1] and DØ[2] experiments in 1995, several of its properties could be deduced from those of its weak partner, the bottom quark. The increment in the measured[3] value of $R = \frac{\sigma(e^+e^- \to hadrons)}{\sigma(e^+e^- \to \mu^+\mu^-)}$ at the b threshold agreed with the predicted $\delta R^{SM} = \frac{1}{3}$, confirming $Q^b = -\frac{1}{3}$. Likewise, data[4] on the front-back asymmetry for electroweak b-quark production confirmed that $T_3^b = -\frac{1}{2}$. Therefore, the b quark's weak partner in the SM was required to be a color-triplet, spin-$\frac{1}{2}$ fermion with electric charge $Q = \frac{2}{3}$ and weak charge $T_3 = \frac{1}{2}$.

Such a particle is readily pair-produced by QCD processes involving $q\bar{q}$ annihilation or gluon fusion. At the Tevatron's $\sqrt{s} = 1.8 - 2.0$ TeV, a 175 GeV top quark is produced 90% through $q\bar{q} \to t\bar{t}$ and 10% through $gg \to t\bar{t}$; at the LHC with $\sqrt{s} = 14$ TeV, the opposite will be true. Eventually, a Linear Collider (LC) with $\sqrt{s} \sim 350$ GeV can operate as a top factory.

In Run I, each Tevatron experiment measured some top quark properties in detail and took a first look at others. As discussed in the next section, our understanding of top as a distinct entiety is rooted in these measurements.

2 Experimental Roots

2.1 Mass

The top quark mass has been measured[5,6] by reconstructing the decay products of top pairs produced at the Tevatron; the best precision comes from the lepton + jets decay channel. The combined measurement from CDF and DØ is $m_t = 174.3 \pm 5.1$ GeV. This implies the Yukawa coupling $\lambda_t = 2^{3/4} G_F^{1/2} m_t$ is ~ 1, the only observed Yukawa coupling of "natural" size.

The high precision with which the m_t is known (comparable to that of m_b and better than that for light quarks [7]) is useful because radiative corrections to many precision electroweak observables are sensitive to m_t. Comparing the experimental constraints on M_W and m_t with the SM prediction[8] for $M_W(m_t, m_{Higgs})$ tests the consistency of the SM. As Figure 1 shows, the data are suggestive, but not able to provide a tightly-bounded value for

* Talk presented at HCP2002, Karlsruhe, Germany, October 2002.

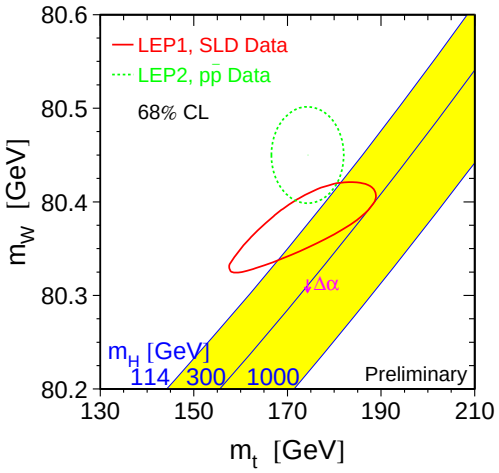

Fig. 1. Predicted[8] $M_W(m_h, m_t)$ in the SM compared[9] to data on M_W, m_t.

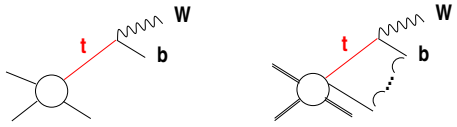

Fig. 2. (left)Top production and decay. (right) Same, with b-quark hadronization indicated. After ref. [11].

m_{Higgs}. Run II measurements of the W and top masses are expected[10] to yield $\delta M_W \approx 40$ MeV (per experiment) and $\delta m_t \approx 3$ GeV (1 GeV in Run IIb or LHC). This should provide a much tighter bound[10] on the SM Higgs mass: $\delta M_H / M_H \leq 40\%$.

A measurement with $\delta m_t \approx 150$ MeV, can in principle be extracted from near-threshold LC[12] data on $\sigma(e^+e^- \to t\bar{t})$. The calculated line shape rises at the remnant of what would have been the toponium 1S resonance (see 2.2). The location of the rise depends on m_t; the shape and size, on the decay width Γ_t. This technique has the potential for high precision because it relies on counting color-singlet $t\bar{t}$ events, making it insensitive to QCD uncertainties.

The definition of m_t used to extract information from this data must be chosen with care. Consider, for example, the mass in the propagator $D(\not{p}) = i/(\not{p} - m_R - \Sigma(\not{p}))$. In principle, one can reconstruct this mass from the four-vectors of the top decay products, as is done in the Tevatron measurements. But this pole mass is inherently uncertain to $\mathcal{O}(\Lambda_{QCD})$. The top production and decay process sketched in Figure 2(left) is, in reality, complicated by

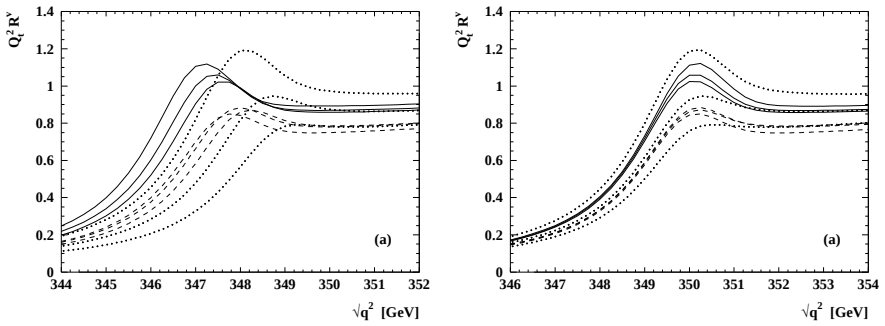

Fig. 3. Near-threshold cross-section for photon-induced top production at an NLC[13] calculated (left) in the pole mass scheme and (right) in the 1S mass scheme. Leading-order (dotted), NLO (dashed) and NNLO (solid) curves are shown with renormalization scales $\mu = 15$ (topmost), 30, and 60 GeV

QCD hadronization effects which connect the b-quark from top decay to other quarks involved in the original scattering,[11] as in Figure 2(right).

Using a short-distance mass definition avoids these difficulties. A convenient choice is the 1S mass[13] $m_{1S} = m_{pole} - \frac{2}{9}\alpha_s^2 m_{pole} + ...$ where $2m_{1S}$ is naturally near the peak of $\sigma(e^+e^- \to t\bar{t})$. Figure 3 compares the photon-induced $t\bar{t}$ cross-section near threshold as calculated in the pole mass and 1S mass schemes (for $m_t = 175$ GeV and $\Gamma_t = 1.43$ GeV). In the pole mass scheme, the location and height of the peak vary with renormalization scale and order in perturbation theory. Using the short-distance mass renders the peak location stable and large higher-order corrections are avoided.

2.2 Top Width and Decays

`top decay width`

In the 3-generation SM, data on the lighter quarks combined with CKM matrix unitarity implies[7] $0.9991 < |V_{tb}| < 0.9994$. Thus the top decays almost exclusively through $t \to Wb$. SM calculations including m_b, m_W and radiative corrections yield [15] $\Gamma_t/|V_{tb}|^2 = 1.42\,\mathrm{GeV}$. As a result, the top decays in $\tau_t \approx 0.4 \times 10^{-24}$ s, a time much less than $\tau_{QCD} \approx 3 \times 10^{-24}$ s. The top quark therefore decays before it can hadronize.

A precise measurement of the top quark width can be made at an LC running at $\sqrt{s} \sim 350$ GeV by exploiting the fact that Γ_t controls the threshold peak height in $\sigma(e^+e^- \to t\bar{t})$. Recent results of NNLL calculations [14] suggest that the theoretical uncertainty will be only $\delta\sigma_{tt}/\sigma_{tt} \approx 3\%$.

`W helicity in top decay`

The SM predicts the fraction ($\mathcal{F}_0$) of top quark decays to longitudinal (zero-helicity) W bosons will be large, due to the top quark's big Yukawa coupling $\mathcal{F}_0 = \frac{m_t^2/2M_W^2}{1+m_t^2/2M_W^2} = (70.1 \pm 1.6)\%$. One can measure $\mathcal{F}_0$ in dilepton

or lepton+jet events by exploiting the correlation of the W helicity with the momentum of the decay leptons: a positive-helicity W (boosted along its spin) yields harder charged leptons than a negative-helicity W.

CDF has measured[16] the lepton p_T spectra for dilepton and lepton + jet events. By assuming no positive-helicity W's are present, CDF obtains the limit $\mathcal{F}_0 = 0.91 \pm 0.37 \pm 0.13$ (i.e., no more than 100% of the W's are longitudinal). By setting $\mathcal{F}_0$ to its SM value of 0.70, they obtain the 95% c.l. upper limit $\mathcal{F}_+ < 0.28$ (i.e., no more than $1 - \mathcal{F}_0$ have positive helicity). More informative constraints are expected from Run II (see Table 1).

b `quark decay fraction`

The top quark's decay fraction to b quarks be measured by CDF[17] to be $B_b \equiv \Gamma(t \to bW)/\Gamma(t \to qW) = 0.99 \pm 0.29$. In the three-generation SM,

$$B_b \equiv \frac{|V_{tb}|^2}{|V_{tb}|^2 + |V_{ts}|^2 + |V_{td}|^2} \,. \tag{1}$$

Three-generation unitarity dictates that the denominator of (1) is 1.0, so that the measurement of B_b implies[17] $|V_{tb}| > 0.76$ at 95% c.l. However, within the 3-generation SM, data on the light quarks combined with CKM unitarity has already provided[7] the much tighter constraints $0.9991 < |V_{tb}| < 0.9994$.

If we add a fourth generation of quarks, the analysis differs. DØ has constrained[7] any 4-th generation b' quark to have a mass greater than $m_t - m_W$; i.e., top cannot decay to b'. Then (1) remains valid, but the denominator of the RHS no longer need equal 1.0. The CDF measurement of B_b now implies $|V_{tb}| \gg |V_{td}|$, $|V_{ts}|$, a stronger constraint than that available [7] from 4-generation CKM unitarity: $0.05 < |V_{tb}| < 0.9994$.

Direct measurement of $|V_{tb}|$ in single top-quark production (via $q\bar{q} \to W* \to t\bar{b}$ and $gW \to t\bar{b}$ as in Figure 7) at the Tevatron should reach an accuracy[18] of 10% in Run IIa (5% in Run IIb).

`FCNC decays`

CDF[19] and ALEPH[20] have set complementary limits on the flavor-changing neutral decays $t \to \gamma q$ and $t \to Zq$ as shown in 4. Run II will provide increased sensitivity to these channels[18] as indicated in Table 2.

2.3 Pair Production

The top pair production cross-section has been measured by CDF[21] and DØ[22], again, most precisely in the lepton + jets channel. The combined

Table 1. Predicted[18] precision of Run II W helicity results for several $\int \mathcal{L}dt$.

	1 fb^{-1}	10 fb^{-1}	100 fb^{-1}
$\delta\mathcal{F}_0$	6.5%	2.1%	0.7%
$\delta\mathcal{F}_+$	2.6%	0.8%	0.3%

Table 2. Run II sensitivity[18] to FCNC top decays as a function of $\int \mathcal{L}dt$.

	1 fb^{-1}	10 fb^{-1}	100 fb^{-1}
$BR(t \to Zq)$	0.015	3.8×10^{-3}	6.3×10^{-4}
$BR(t \to \gamma q)$	3.0×10^{-3}	4.0×10^{-4}	8.4×10^{-5}

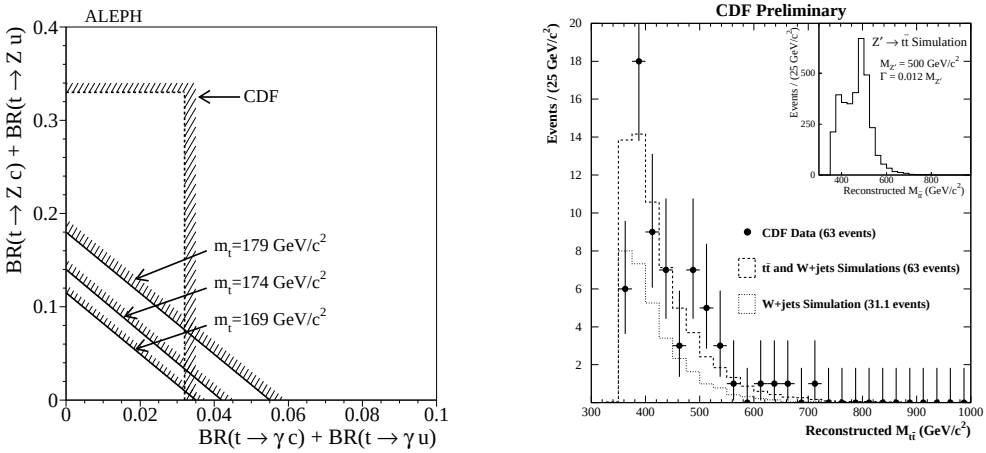

Fig. 4. (left) FCNC limits from CDF [19]and ALEPH[20]. (right) CDF [24] limits on leptophobic Z'

average of $\sigma_{tt}(m_t = 172\,\text{GeV}) = 5.9 \pm 1.7$ pb is consistent with SM predictions including radiative corrections.[23]

Initial measurements of the invariant mass (M_{tt}) and transverse momentum (p_T) distributions of the produced top quarks have yielded preliminary limits on new physics. As seen in figure 4, e.g., a narrow 500 GeV Z' boson is inconsistent with the observed shape of CDF's M_{tt} distribution.[24]

In Run II, the σ_{tt} measurement will be dominated by systematic uncertainties; the large data sample will be used to reduce reliance on simulations.[18] An integrated luminosity of 1 (10, 100) fb^{-1} should [18] enable σ_{tt} to be measured to $\pm$ 11 (6, 5) %. The M_{tt} distribution will then constrain $\sigma \cdot B$ for new resonances decaying to $t\bar{t}$ as illustrated in Figure 5.

2.4 Spin Correlations

When a $t\bar{t}$ pair is produced, the spins of the two fermions are correlated.[25] Because the top quark decays before its spin can flip,[26] the spin correlations between t and $\bar{t}$ yield angular correlations among their decay products. If χ is angle between the top spin and the momentum of a given decay product,

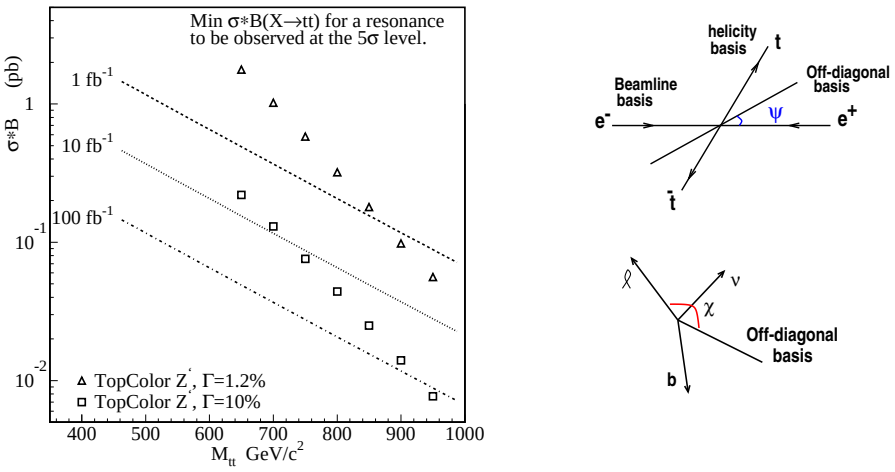

Fig. 5. (left)Anticipated[18] Run II limits on $\sigma \cdot B(X \to t\bar{t})$ (right) Definitions of the off-diagonal basis and decay lepton angles for studying top spin correlations.

the differential top decay rate (in the top rest frame) is

$$\frac{1}{\Gamma}\frac{d\Gamma}{d\cos\chi} = \frac{1}{2}(1 + \alpha\cos\chi) \tag{2}$$

The factor α is [27] 1.0 (0.41, -0.31, -0.41) if the decay product is ℓ or d (W, ν or u, b). Thus, dilepton events are best for studying $t\bar{t}$ spin correlations.

At the Tevatron, spin correlations are best studied in an optimal "off-diagonal" basis[28,29] in which the spins are purely anti-correlated at leading order $(t_\uparrow \bar{t}_\downarrow + t_\downarrow \bar{t}_\uparrow)$. The projection axis is identified by angle ψ

$$\tan\psi = \frac{\beta^2 \sin\theta^* \cos\theta^*}{1 - \beta^2 \sin^2\theta^*} \tag{3}$$

where β ($\theta*$)is the top quark's speed (scattering angle) in the center-of-momentum scattering frame (see Figure 5). Writing the differential cross-section in terms of the angles $\chi^\pm$ of the decay leptons $\ell^\pm$,

$$\frac{1}{\sigma}\frac{d^2\sigma}{d(\cos\chi_+)d(\cos\chi_-)} = \frac{1}{4}(1 + \kappa\cos\chi_+\cos\chi_-) \tag{4}$$

one finds $\kappa \approx 0.9$ in the SM for $\sqrt{s} = 1.8$ TeV. DØ used the six Run I dilepton events to set[30] the 68% c.l. limit $\kappa \geq -0.25$. Run IIa promises $\sim$150 dilepton events.[18]

At the LHC, the top dilepton sample will be of order 4×10^5 events per year[15] – but no spin basis with nearly 100% correlation at all β has been identified. Near threshold, angular momentum conservation favors like helicities; far above threshold, helicity conservation favors opposite helicities.[15]

Spin effects in single top production at LHC are also under study. Promising variables include the angles between the initial d and decay e (in the $W*$ process or Wg fusion - see Figure 7) or the angles between the e^+ from top decay and the $e-$ from W decay (in $gb \to tW$).

3 Branches of Theory

We now explore how top influences some branches of theory beyond the SM. The small Run I top sample leaves open many intriguing possibilities.

3.1 Light Neutral Higgs in MSSM

Radiative corrections to m_h involving virtual top quarks introduce a dependence on m_t; the heavy top makes these significant[31] . For $\tan\beta > 1$,

$$M_h^2 < M_Z^2 \cos^2(2\beta) + \frac{3G_f}{\sqrt{2}\pi^2}\ m_t^4\ ln\left(\frac{\tilde{m}^2}{m_t^2}\right) \tag{5}$$

Including higher-order corrections, the most general limit appears to be $M_h <$ 130 GeV, well above the current bounds but in reach of upcoming experiment. This is comparable to the generic SUSY limit $M_h < 150$ GeV from requiring the Higgs self-coupling to be perturbative up to M_{Planck}. [31]

3.2 Charged Higgs

Models from SUSY to dynamical symmetry breaking [32] include light charged scalar bosons, into which top may decay: $t \to H^+ b$. If $m_H^\pm < m_t - m_b$, the decay $t \to H^+ b$ competes with the standard decay mode $t \to Wb$. Since the $tbH^\pm$ coupling depends on $\tan\beta$ as[33][$m_t \cot\beta(1+\gamma_5) + m_b \tan\beta(1-\gamma_5)$], the additional decay mode is significant for either large or small values of $\tan\beta$. The charged scalar decays as $H^\pm \to cs$ or $H^\pm \to t^* b \to Wbb$ if $\tan\beta$ is small and as $H^\pm \to \tau\nu_\tau$ if $\tan\beta$ is large. The final state reached through an intermediate $H^\pm$ will cause the original $t\bar{t}$ event to fail the usual cuts for the lepton + jets channel. A reduced rate in this channel signals the presence of a charged scalar. Expected DØ limits in run II are shown in Figure 6.

3.3 Sfermion Masses

SUSY models must explain why the scalar Higgs boson acquires a negative mass-squared (breaking the electroweak symmetry) while the scalar fermions do not (preserving color and electromagnetism). In the MSSM with GUT unification or models with dynamical SUSY breaking, the answer involves the heavy top quark.[31] In these theories, the masses of the Higgs bosons and sfermions are related at a high energy scale M_χ:

$$M_{h,H}^2(M_\chi) = m_0^2 + \mu^2 \qquad\qquad M_{\tilde{f}}^2(M_\chi) = m_0^2 \tag{6}$$

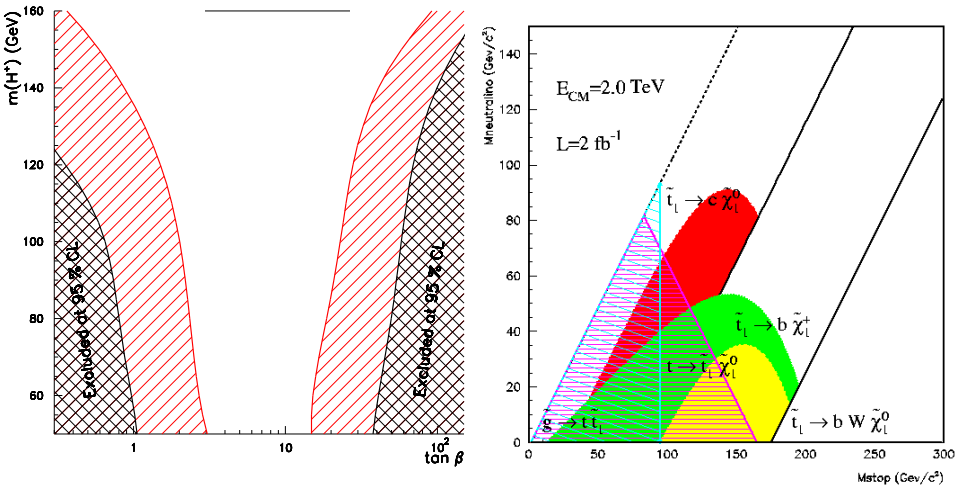

Fig. 6. Projected DØ reach in Run II searches for (left) charged scalars in $t \to H^{\pm} b$ [34] assuming $\sqrt{s} = 2$ TeV, $\int \mathcal{L} dt = 2\text{fb}^{-1}$, and $\sigma(t\bar{t}) = 7\text{pb}$ (right) stop searches in various channels.[38]

where the squared masses are all positive so that the vacuum preserves the color and electroweak symmetries. Renormalization group running yields scalar masses at lower energies.[35] At scale q, the solution for M_h is, e.g.,

$$M_h^2(q) \approx M_h^2(M_X) - \frac{3}{8\pi^2}\lambda_t^2\Big(\tilde{M}_{Q_L^3}^2 + \tilde{M}_{t_R}^2 + M_h^2 + A_{o,t}^2\Big) ln\left(\frac{M_X}{q}\right) \qquad (7)$$

and the top Yukawa coupling λ_t is seen to be reducing M_h^2. For $m_t \sim 175$ GeV, this effect drives only the Higgs mass negative, just as desired.[36]

SUSY models include bosonic partners for t_L and t_R. The mass-squared matrix for the top squarks [31] (in the $\tilde{t}_L, \tilde{t}_R$ basis)

$$\tilde{m}_t^2 = \begin{pmatrix} \tilde{M}_Q^2 + m_t^2 & m_t(A_t + \mu \cot\beta) \\ +M_Z^2(\frac{1}{2} - \frac{2}{3}\sin^2\theta_W)\cos 2\beta & \\ m_t(A_t + \mu\cot\beta) & \tilde{M}_U^2 + m_t^2 \\ & +\frac{2}{3}M_Z^2 \sin^2\theta_W \cos 2\beta \end{pmatrix} \qquad (8)$$

has off-diagonal entries proportional to m_t. Hence, a large m_t can drive one of the top squark mass eigenstates to be relatively light. Experiment still allows a light stop,[37]; Run II will be sensitive to higher stop masses in several decay channels[38] (Figure 6).

Perhaps some of the Run I "top" sample included top squarks.[39] If $m_{\tilde{t}} > m_t$, perhaps $\tilde{t}\bar{\tilde{t}}$ production occurred in Run I, with the top squarks decaying to top plus $\tilde{N}$ or $\tilde{g}$ (depending on the masses of the gauginos). If

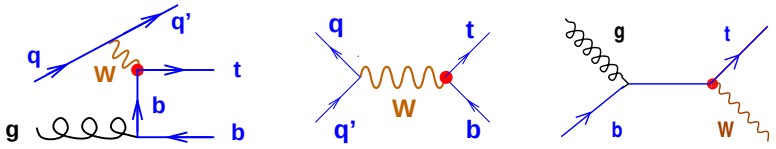

Fig. 7. Feynman diagrams for single top quark production.

$m_t > m_{\tilde{t}}$ some top quarks produced in $t\bar{t}$ pairs in Run I may have decayed to top squarks via $t \to \tilde{t}\tilde{N}$ with the top squarks' decay being either semi-leptonic $\tilde{t} \to b\ell\tilde{\nu}$ or flavor-changing $\tilde{t} \to c\tilde{N}, c\tilde{g}$. Or maybe gluino pair production occurred, followed by $\tilde{g} \to t\tilde{t}$. These ideas can be tested using the rate, decay channels, and kinematics of top quark events.[40]

3.4 Extra EW gauge bosons

Many models of physics beyond the SM include extended electroweak gague groups coupled differently to the third generation fermions (h) than to the light fermions (ℓ). Examples include superstring theories with flavor U(1) groups and dynamical symmetry breaking models with an extra SU(2) to produce m_t or an extra U(1) to explain $m_t - m_b$.

When the high-energy $SU(2)_h \times SU(2)_\ell \times U_1(Y)$ or $SU(2)_W \times U(1)_h \times U(1)_\ell$ group breaks to electromagnetism, the resulting gauge boson mass eigenstates are [41] heavy states W^H, Z^H that couple mainly to the third generation, light states W^L, Z^L resembling the standard W and Z, and a massless photon $A^\mu = \sin\theta[\sin\phi\, W^\mu_{3\ell} + \cos\phi\, W^\mu_{3h}] + \cos\theta X^\mu$ coupling to $Q = T_{3h} + T_{3\ell} + Y$. Here, ϕ describes the mixing between the original two weak or hypercharge groups and θ is the usual weak angle.

There are several ways to test whether the high-energy weak interactions have the form $SU(2)_h \times SU(2)_\ell$. One possibility is to search for the extra weak bosons. Low-energy exchange of Z^H and W^H bosons would cause apparent four-fermion contact interactions; LEP limits on $eebb$ and $ee\tau\tau$ contact terms imply[42] $M_{Z^H} \gtrsim 400$ GeV. Direct production of Z^H and W^H at Fermilab is also feasible; a Run II search for $Z^H \to \tau\tau \to e\mu X$ will be sensitive[42] to Z^H masses up to 750 GeV. Precision electroweak data suggest that $M_{W^H, Z^H} \geq 2$ TeV if no other physics cancels the bosons' effects. Another possibility is to measure the top quark's weak interactions in single top production. Run II should measure the ratio of single top and single lepton cross-sections $R_\sigma \equiv \sigma_{tb}/\sigma_{\ell\nu}$ to $\pm 8\%$ in the W^* process.[43] making the experiments sensitive[44] to W^H bosons up to masses of about 1.5 TeV.

There are likewise several ways to seek evidence for a $U(1)_h \times U(1)_\ell$ structure. CDF specifically [24] excludes a leptophobic topcolor Z' decaying to $t\bar{t}$ if $M \leq 480$ (780) GeV assuming $\Gamma/M = 0.012$ (0.04). Precision electroweak data constrains[45] flavor non-universal Z' bosons to have masses in excess of

1-2 TeV if no other physics cancels their effects. As mentioned earlier, FNAL Run II will be directly sensitive[42] to Z' bosons as heavy as 750 GeV via $Z' \to \tau\tau \to e\mu X$. A high-energy LC would be capable of finding a 3-6 TeV Z' decaying to taus.[46]

3.5 New Top Strong Interactions

If the top quark feels a new strong interaction, a top condensate may be involved in electroweak symmetry breaking. Consider, e.g., an extended 'top-color' gauge structure[47]: $SU(3)_h \times SU(3)_\ell \to SU(3)_{QCD}$ where t and b transform under $SU(3)_h$ and the light quarks, under $SU(3)_\ell$. Below the symmetry-breaking scale M, the spectrum includes massive topgluons which mediate vectorial color-octet interactions among top quarks: $-(4\pi\kappa/M^2)(\bar{t}\gamma_\mu \frac{\lambda^a}{2} t)^2$. If the coupling κ lies above a critical value ($\kappa_c = 3\pi/8$ in the NJL[48] approximation), a top condensate forms. For a second-order phase transition, $\langle \bar{t}t \rangle / M^3 \propto (\kappa - \kappa_c)/\kappa_c$, so the top quark mass generated by this dynamics can lie well below the symmetry breaking scale.

Models with strong top dynamics form three classes, whose distinctive spectra and phenomenology we now review: topcolor,[47,49] flavor-universal extended color,[46] and top seesaw.[50]

`Topcolor Models`

Topcolor[47,49] models include extended color and hypercharge sectors and a standard weak gauge group. The third-generation fermions transform under the more strongly-coupled $SU(3)_h \times U(1)_h$ group, so that after the extended symmetry breaks to the SM gauge group the heavy topgluons and Z' couple preferentially to the third generation. The light fermions transform under $SU(3)_\ell \times U(1)_\ell$. CDF's search[51] for topgluons decaying to $b\bar{b}$ excludes 280 (340, 375) GeV $\leq M \leq$ 670 (640, 560) GeV for $\Gamma/M = 0.3$ (0.5, 0.7); the topgluon's strong coupling to quarks makes it broad. Run II and the LHC should be sensitive to topgluons in $b\bar{b}$ or $t\bar{t}$ final states.

Because the topgluon and Z' couple differently to quarks in different generations, they contribute to flavor-changing neutral currents. Data on neutral B-meson mixing, e.g., implies [52] $M_c >$ 3-5 TeV and $M_{Z'} >$ 7-10 TeV.

The strong topcolor dynamics binds top and bottom quarks into a set of top-pions[47,49] $t\bar{t}, t\bar{b}, b\bar{t}$ and $b\bar{b}$. A singly-produced neutral top-higgs can be detected[53] through its flavor-changing decays to tc at Run II. Charged top-pions, on the other hand, would be visible[54] in single top production, as in Figure 8, up to masses of 350 GeV at Run II and 1 TeV at LHC.

`Flavor-Universal Coloron Models`

The gauge structure of these models[46] is identical to that of topcolor[47]. The fermion hypercharges are as in topcolor models; hence, the Z' phenomenology is also the same. All quarks transform under the more strongly-coupled $SU(3)_h$ group; none transform under $SU(3)_\ell$. As a result, the heavy coloron bosons in the low-energy spectrum couple with equal strength to all

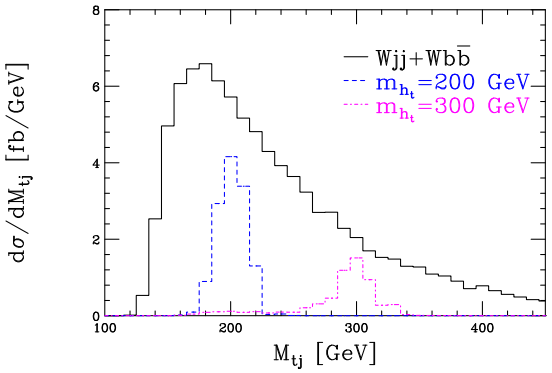

Fig. 8. Simulated signal and background for charged top-pions in the Tevatron's single top sample.[54]

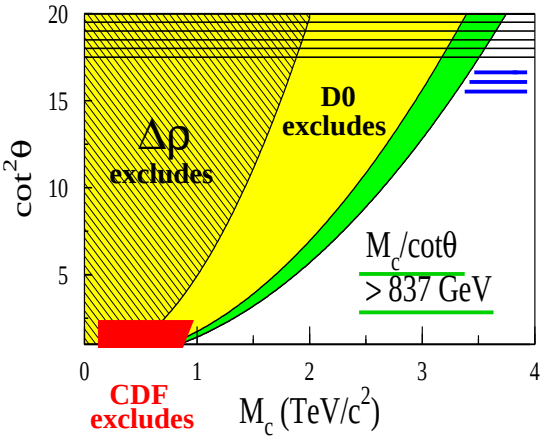

Fig. 9. Limits[55] on the mass and mixing angle of flavor-universal colorons.

quarks. Experimental limits[55] on these color-octet states are shown in Figure 9. The most widely applicable bounds come from the shape of the dijet angular distribution or invariant mass; the current limit is $M_c/\cot\theta > 837$ GeV (θ is the mixing angle between the $SU(3)$ groups). This implies $M_c \gtrsim 3.4$ TeV in dynamical models of mass generation where the coloron coupling is strong.

These models are less constrained by flavor physics than topcolor models because both the colorons and composite pions are flavor-universal. For example, B-meson mixing places only weak bounds on the Z' mass [56].

`Top Seesaw Models`

Table 3. Third generation quark charge assignments in top seesaw models.[50]

	$SU(3)_h$	$SU(3)_\ell$	$SU(2)$
$(t,\, b)_L$	3	1	2
$t_R,\ b_R$	1	3	1
χ_L	1	3	1
χ_R	3	1	1

Top seesaw models[50] include an extended $SU(3)_h \times SU(3)_\ell$ color group and a standard electroweak group. In addition to the ordinary quarks, new weak-singlet quarks χ mix with top. The color and weak quantum numbers of the third-generation quarks are shown in Table 3. When the $SU(3)_h$ coupling becomes strong, a dynamical top mass is created through a combination of $t_L \chi_R$ condensation and seesaw mixing:

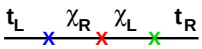

$$\left(\bar{t}_L\ \bar{\chi}_L\right) \begin{pmatrix} 0 & m_{t\chi} \\ \mu_{\chi t} & \mu_{\chi\chi} \end{pmatrix} \begin{pmatrix} t_R \\ \chi_R \end{pmatrix} \tag{9}$$

Composite scalars $\bar{t}_L \chi_R$ are also created by the strong dynamics.

A combination of precision electroweak bounds and triviality considerations limits the χ quarks to have masses $\gtrsim$ 5 TeV. [57,58] Direct searches for weak-singlet quarks are limited to lower mass ranges, making them sensitive to weak-singlet partners of the lighter quarks. For example, a heavy mostly-weak-singlet quark q^H could contribute[59] to the FNAL top dilepton sample via $p\bar{p} \to q^H \bar{q}^H \to q^L W \bar{q}^L W \to q^L \bar{q}^L \ell\nu_\ell \ell'\nu_{\ell'}$ Run 1 data places the limit[59] $M_{s^H,d^H} \gtrsim 140$ GeV, but cannot directly constrain M_{b^H}. In models where all three generations of quarks have weak-singlet partners, self-consistency requires[59] $M_{b^H} \gtrsim 160$ GeV.

4 Summary

The puzzles of electroweak symmetry breaking and fermion masses require physics beyond the SM for their solution. Thus, the top quark may have visibly unusual attributes such as new gauge interactions or decay channels, exotic fermion partners, a light supersymmetric partner, or even strongly-bound top-quark states. Our field needs new surprising data, and hadron collider studies of top may soon provide it!

Acknowledgments

This work was supported in part by the U.S. Department of Energy under grant DE-FG02-91ER40676

References

1. F. Abe *et al.*, *Phys. Rev. Lett* **74**, 2662 (1995)
2. S. Abachi *et al.*, *Phys. Rev. Lett* **74**, 2632 (1995)
3. E. Rice *et al.*, *Phys. Rev. Lett* **48**, 906 (1982)
4. W. Bartel *et al.*, *Phys. Lett.*B **146**, 437 (1984)
5. F. Abe *et al. Phys. Rev. Lett* **80**, 2767 (1998); *Phys. Rev. Lett* **80**, 2779 (1998); *Phys. Rev. Lett* **82**, 271 (1999)
6. S. Abachi *et al. Phys. Rev. Lett* **79**, 1197 (1997); B. Abbott *et al. Phys. Rev. Lett* **80**, 2063 (1998); *Phys. Rev.*D **58**, 052001 (1998); *Phys. Rev.*D **60**, 052001 (1999)
7. D.E. Groom *et al.*, *E. Phys. J.* C **C15**, 1 (2000)
8. G. Degrassi, *et al.*, *Phys. Lett.*B **418**, 209 (1998)
9. LEP Electroweak Working Group, http://lepewwg.web.cern.ch/LEPEWWG/
10. G. Watts, Talk given at Heavy Flavours 8, Southampton, England, July 25-29, 1999. http://www-d0.fnal.gov/∼gwatts/outside/hf8/
11. M.C. Smith and S.S. Willenbrock, *Phys. Rev. Lett* **79**, 3825 (1997)
12. P. Comas *et al.*, Recent Studies on Top Quark Physics at NLC, Proc. Iwate Linear Colliders, eds. A. Miyamoto, Y. Fujii, T. Matsui, and S. Iwata (World Scientific, 1996), p. 455.
13. A.H. Hoang and T. Teubner, *Phys. Rev.*D **60**, 114027 (1999)
14. A. H. Hoang, A. V. Manohar, I. W. Stewart and T. Teubner, *Phys. Rev.*D **65**, 014014 (2002)
15. M. Beneke *et al.*, Top Quark Physics, hep-ph/0003033.
16. T. Affolder *et al.*, *Phys. Rev. Lett* **84**, 216 (2000)
17. K. Tollefson, CDF Collaboration, Fermilab-Conf-98/389-E, 1998.
18. D. Amidei and R. Brock, eds., Future ElectroWeak Physics at the Fermilab Tevatron: Report of the TeV2000 Study Group, Fermilab-Pub-96/046. http://www-theory.fnal.gov/TeV2000.html .
19. F. Abe *et al.*, *Phys. Rev. Lett* **80**, 2525 (1998)
20. A. Heister *et al.* hep-ex/0206070 ; CERN-EP-2002-042.
21. F. Abe *et al.*, *Phys. Rev. Lett* **80**, 2773 (1998)
22. S. Abachi *et al.*, *Phys. Rev. Lett* **79**, 1203 (1997)
23. E. Laenen, J. Smith, and W.L. van Neerven, *Phys. Lett.*B **321**, 254 (1994); E. Berger and H. Contopangonos, *Phys. Rev.*D **57**, 253 (1998); R. Bociani *et al.*, *Nucl. Phys.*B , 5 (2)94241998
24. T. Affolder *et al.*, *Phys. Rev. Lett* **85**, 2062 (2000)
25. V. Barger, J. Ohnemus, and R. Phillips, *Int. J. Mod. Phys.* A **4**, 617 (1989)
26. I. Bigi *et al.*, *Phys. Lett.*B **181**, 157 (1986)
27. M. Jezabek and J.H. Kuhn, *Phys. Lett.*B **329**, 317 (1994)
28. S. Parke and Y. Shadmi, *Phys. Lett.*B **387**, 199 (1996)
29. G. Mahlon and S. Parke, *Phys. Lett.*B **411**, 173 (1997)
30. B. Abbott *et al.*, *Phys. Rev. Lett* **85**, 256 (2000)
31. For a review of supersymmetry, consult: H. Murayama in the TASI 2000 lectures; or S. Dawson, SUSY and Such, hep-ph/9712464.
32. For a review of dynamical electroweak symmetry breaking, consult: C.T. Hill and E.H. Simmons, hep-ph/0203079 .
33. For a review, see J. Gunion *et al.* The Higgs Hunter's Guide, (Addison-Wesley, 1990).

34. S. Snyder, Proc. EPS-HEP 99, Tampere, Finland, 15-21 July 1999, hep-ex/9910029.
35. M. Machacek and M. Vaughn, *Nucl. Phys.*B **222**, 83 (1983); C. Ford *et al.*, *Nucl. Phys.*B **395**, 17 (1993)
36. V. Barger, M. Berger and P. Ohmann, *Phys. Rev.*D **49**, 4908 (1994)
37. T. Affolder *et al.*, *Phys. Rev. Lett* **84**, 5704 (2000); *Phys. Rev. Lett* **84**, 5273 (2000)
38. R. Demina *et al.*, *Phys. Rev.*D **62**, 035011 (2000)
39. G.L. Kane and S. Mrenna, *Phys. Rev. Lett* **77**, 3502 (1996); G. Mahlon and G.L. Kane, *Phys. Rev.*D **55**, 2779 (1997); M. Hosch *et al.*, *Phys. Rev.*D **58**, 034002 (1998)
40. See, for example, the "experimental symptoms of new top physics" list located at http://b0nd10.fnal.gov/∼regina/thinkshop/ts.html
41. R.S. Chivukula, E.H. Simmons, and J. Terning, *Phys. Lett.*B **331**, 383 (1994)
42. K.R. Lynch, *et al.*, *Phys. Rev. D* to appear. hep-ph/0007286
43. A.P. Heinson, Proc. 31st Rencontres de Moriond, Les Arcs, France, March 23-30, 1996; A..P. Heinson, A.S. Belyaev and E.E. Boos, *Phys. Rev.*D **56**, 3114 (1997); M.C. Smith and S. Willenbrock, *Phys. Rev.*D **54**, 6696 (1996)
44. E.H. Simmons, *Phys. Rev.*D **55**, 5494 (1997)
45. R. S. Chivukula and E. H. Simmons, Phys. Rev. D **66**, 015006 (2002)
46. R.S. Chivukula, A.G. Cohen, and E.H. Simmons, *Phys. Lett.*B **380**, 92 (1996); M.B. Popovic and E.H. Simmons, *Phys. Rev.*D **58**, 095007 (1998); K. Lane, *Phys. Lett.*B **433**, 96 (1998)
47. C.T. Hill, *Phys. Lett.*B **266**, 419 (1991); S.P. Martin, *Phys. Rev.*D **45**, 4283 (1992); *Phys. Rev.*D **46**, 2197 (1992); *Nucl. Phys.*B **398**, 359 (1993); M. Lindner and D. Ross, *Nucl. Phys.*B **370**, 30 (1992); R. Bonisch, *Phys. Lett.*B **268**, 394 (1991); C.T. Hill *et al.*, *Phys. Rev.*D **47**, 2940 (1993); C.T. Hill, *Phys. Lett.*B **345**, 483 (1995); R.S. Chivukula and H. Georgi, *Phys. Rev.*D **58**, 115009 (1998); *Phys. Rev.*D **58**, 075004 (1998)
48. Y. Nambu and G. Jona-Lasinio, *Phys. Rev.* **122**, 345 (1961) ; *Phys. Rev.* **124**, 246 (1961)
49. R.S. Chivukula, B.A. Dobrescu, and J. Terning *Phys. Lett.*B **353**, 289 (1995); K. Lane and E. Eichten, *Phys. Lett.*B **352**, 382 (1995); K. Lane, *Phys. Rev.*D **54**, 2204 (1996); G. Buchalla *et al*, *Phys. Rev.*D **53**, 5185 (1996); K. Lane, *Phys. Lett.*B **433**, 96 (1998)
50. B.A. Dobrescu and C.T. Hill, *Phys. Rev. Lett* **81**, 2634 (1998); R.S. Chivukula *et al.*, *Phys. Rev.*D **59**, 075003 (1999)
51. F. Abe *et al.*, *Phys. Rev. Lett* **82**, 2038 (1999).
52. G. Burdman, K. D. Lane and T. Rador, *Phys. Lett.*B **514**, 41 (2001)
53. G. Burdman, *Phys. Rev. Lett* **83**, 2888 (1999)
54. H.-J. He and C.P. Yuan, *Phys. Rev. Lett* **83**, 28 (1999)
55. I.A. Bertram and E.H. Simmons, *Phys. Lett.*B **443**, 347 (1998); E.H. Simmons, *Phys. Rev.*D **55**, 1678 (1997)
56. E. H. Simmons, *Phys. Lett.*B **526**, 365 (2002)
57. H. Collins, A. Grant, and H. Georgi, *Phys. Rev.*D **61**, 055002 (2000)
58. R.S. Chivukula and N. Evans, *Phys. Lett.*B **464**, 244 (1999); R.S. Chivukula, N. Evans, and C. Hoelbling, *Phys. Rev. Lett* **85**, 511 (2000)
59. M. Popovic and E.H. Simmons, *Phys. Rev.*D **62**, 035002 (2000)